Electronic Supplementary Material (ESI) for Energy & Environmental Science.
This journal is © The Royal Society of Chemistry 2018

Nacre-inspired crystallization and elastic "brick-and-mortar" structure for a wearable perovskite solar module

Xiaotian Hu[a,b], Zengqi Huang[c], Fengyu Li[*a], Meng Su[a], Zhandong Huang[a,b], Zhipeng Zhao[a,b], Zheren Cai[a,b], Xia Yang[c], Xiangchuan Meng[c], Pengwei Li[a,b], Yang Wang[a], Mingzhu Li[a], Yiwang Chen[3], Yanlin Song[*a]

[a]*Key Laboratory of Green Printing, Institute of Chemistry, Chinese Academy of Sciences (ICCAS), Beijing Engineering Research Center of Nanomaterials for Green Printing Technology, Beijing National Laboratory for Molecular Sciences (BNLMS), Beijing, 100190, P. R. China.*

[b]*University of Chinese Academy of Sciences, Beijing, 100049, P. R. China.*

[c]*College of Chemistry/Institute of Polymers, Nanchang University, Nanchang 330031, P. R. China*

[*]*E-mail: ylsong@iccas.ac.cn & forrest@iccas.ac.cn*

Content

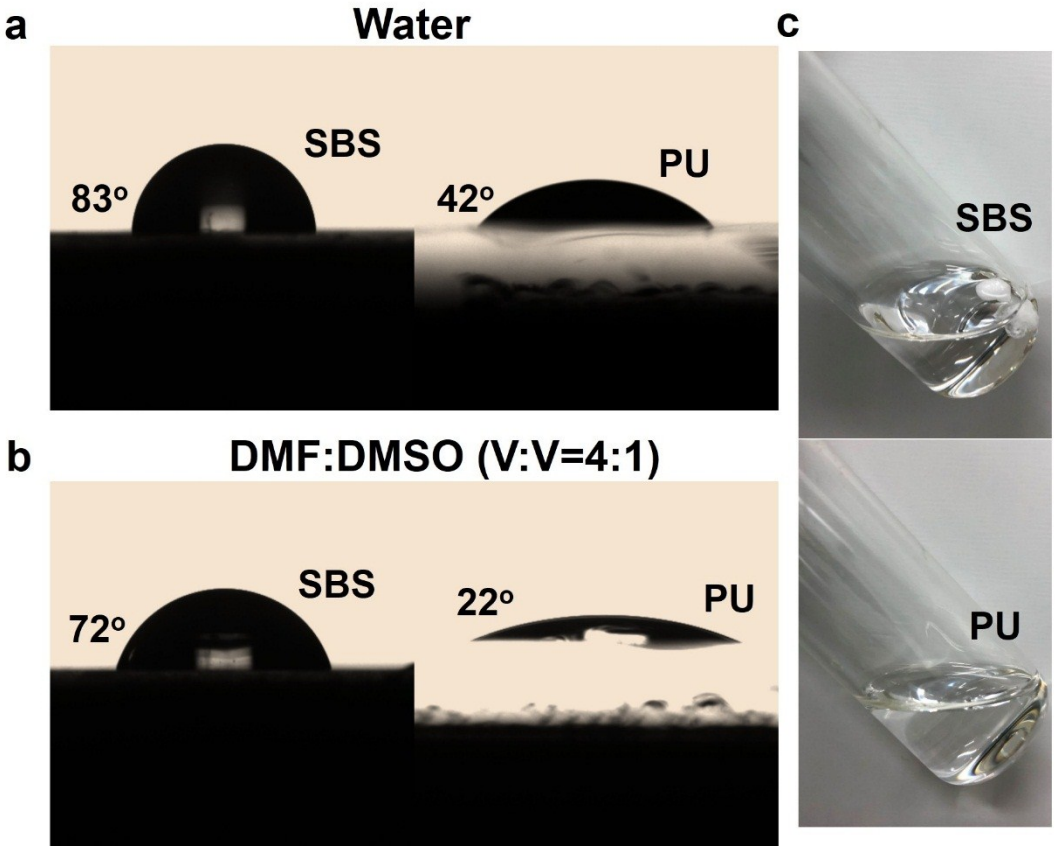

Fig. S1. The contact angle of (a) Water and (b) DMF:DMSO (V:V=4:1) on SBS and PU films, respectively. (c) Photographs of SBS and PU in DMF:DMSO (V:V=4:1) solvent.

The differences in contact angle and photographs of solubility can verify the insoluble property of SBS and soluble property of PU.

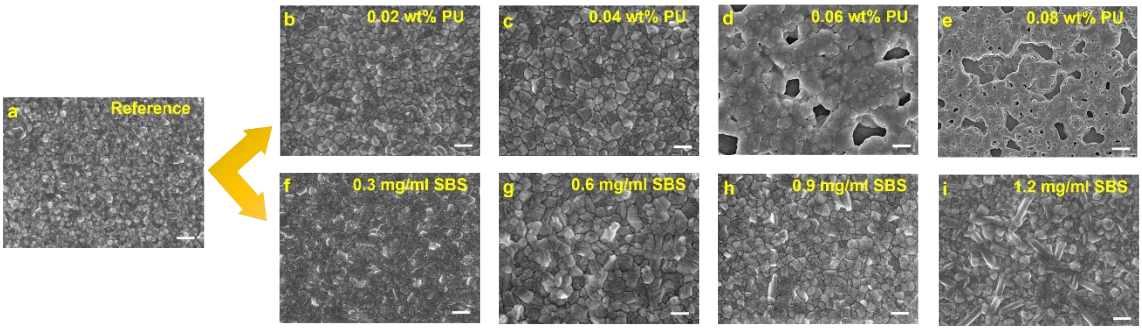

Fig. S2. SEM images of PVK films with different concentrations PU (wt% in precursor solution) or SBS (mg/ml in chlorobenzene anti-solvent) on PDMS/PEDOT:PSS electrode. All the scale bars, 500 nm.

As pervious reported[1], PU can enhance the grain size of PVK due to the retardation of crystal growth. However, it shows obvious voids when the PU concentration over 0.04 wt%, it could be ascribed to excessive interaction between PU with PbX_2 (X = I and Br). Meanwhile, SBS can also enhance the grain size of PVK because the hydrophobic and insoluble properties of SBS can reduce the number of nucleation sites during PVK crystal growth. On the other hand, for C_{SBS} >0.6 mg/ml, excessive SBS could aggregate on the surface. Based on the above results, the concentration of SBS and PU is defined as 0.04 wt% and 0.6 mg/ml in the following discussion.

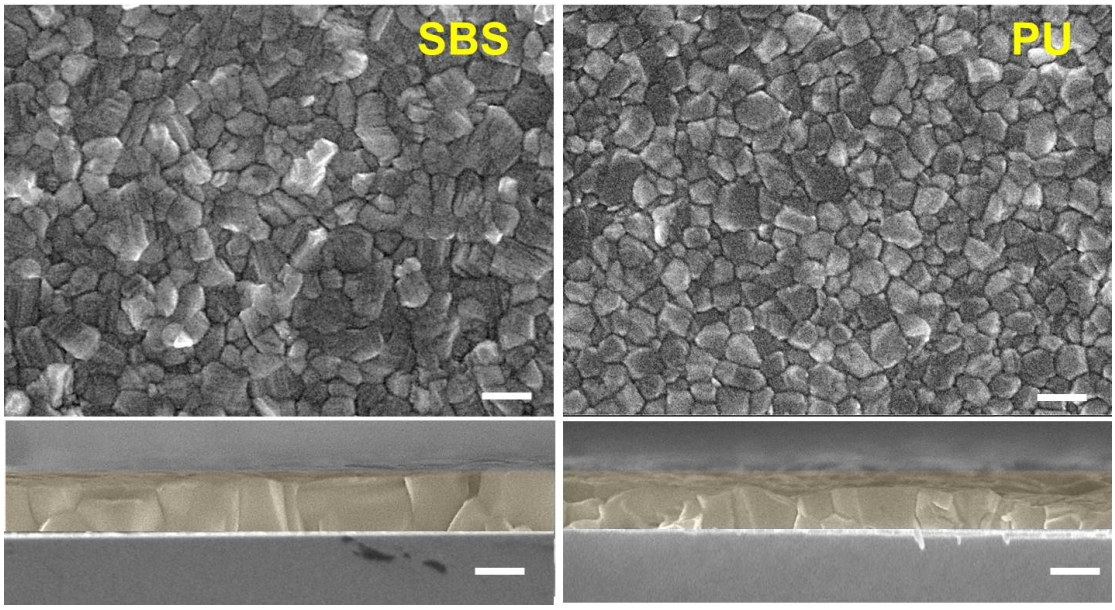

Fig. S3. The top-view and cross-section SEM images of SBS- and PU-based PVK films.

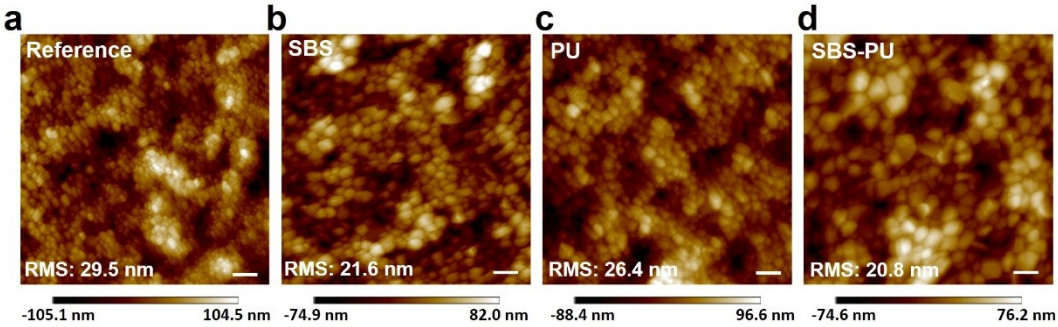

Fig. S4. AFM height images of (a) Reference, (b) SBS-based, (c) PU-based and (d) SBS-PU-based PVK films on PDMS/PEDOT:PSS electrode. All the scale bars, 1μm.

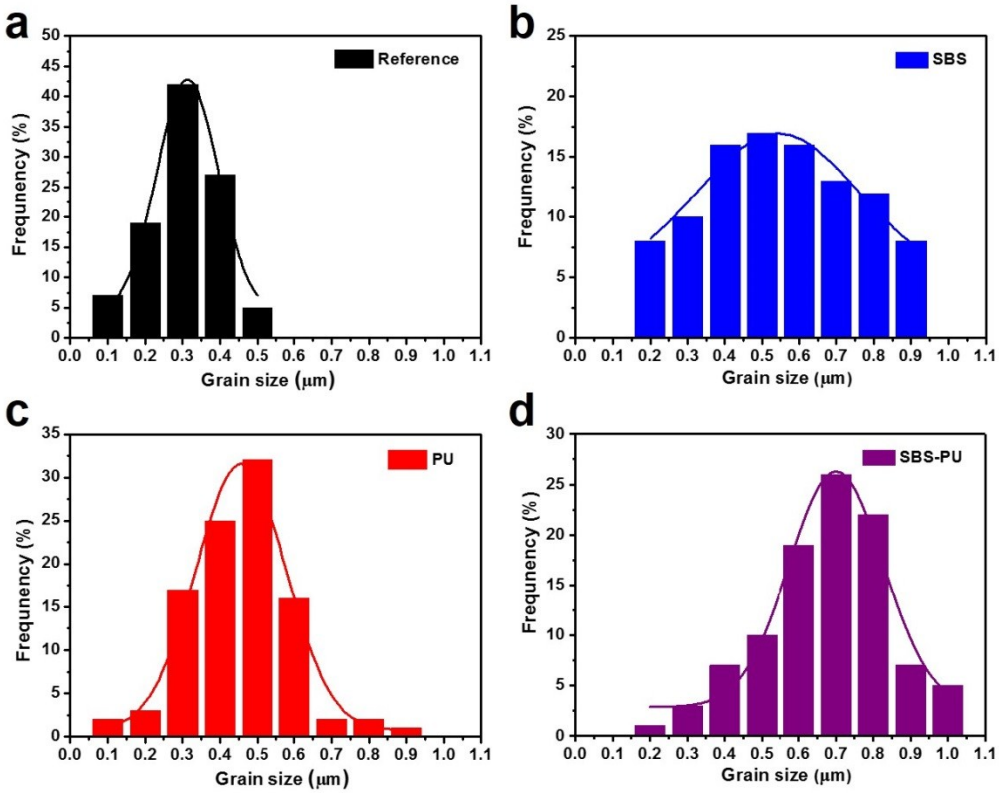

Fig. S5. Histogram of grain-size distributions. (a) Reference, (b) SBS-based, (c) PU-based and (d) SBS-PU-based PVK films on PDMS/PEDOT:PSS electrode.

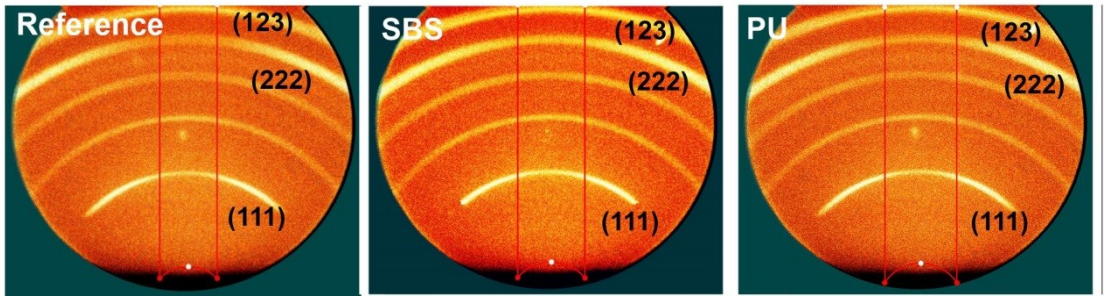

Fig. S6. 2D-XRD images of Reference, SBS- and PU- based PVK films.

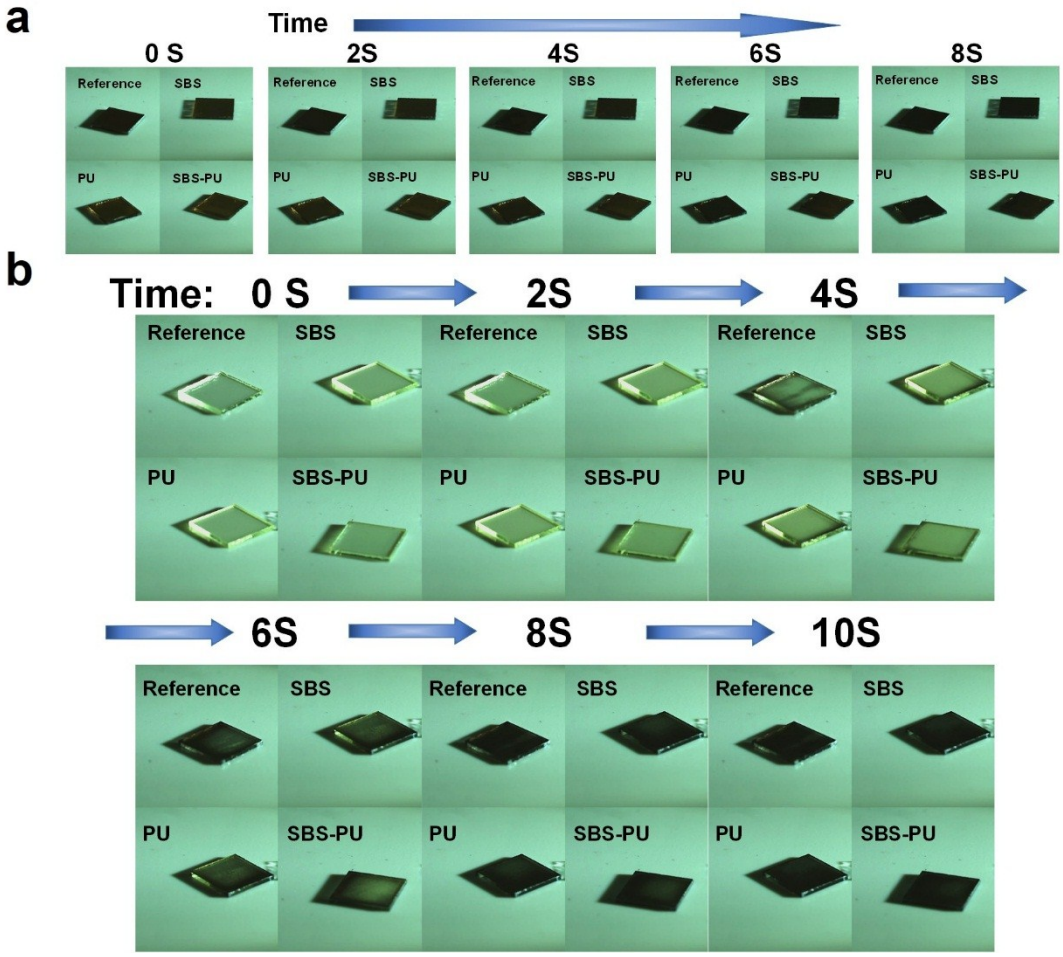

Fig. S7. Photographs of different PVK films on Glass/PDMS/PEDOT:PSS substrate during initial crystallization at 100 ^{o}C via the high-speed camera. (a) standard concentration of PVK precursor solution for PSCs fabrication. (b) 30% standard concentration of PVK precursor solution to demonstrate the phenomenon clearly.

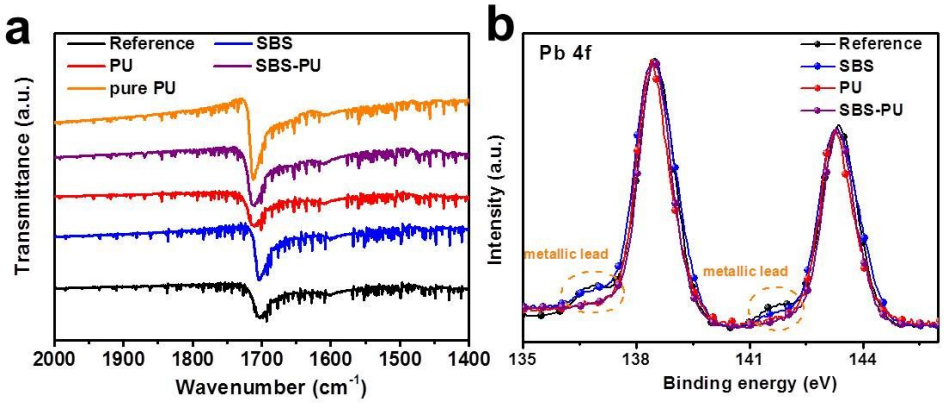

Fig. S8. (a), FTIR spectra of various PVK films on KBr substrate. The C=O stretching vibration bond[2] is at 1710 cm^{-1}. (b), X-ray photoelectron spectroscopy of various PVK films on Glass/ITO substrate.

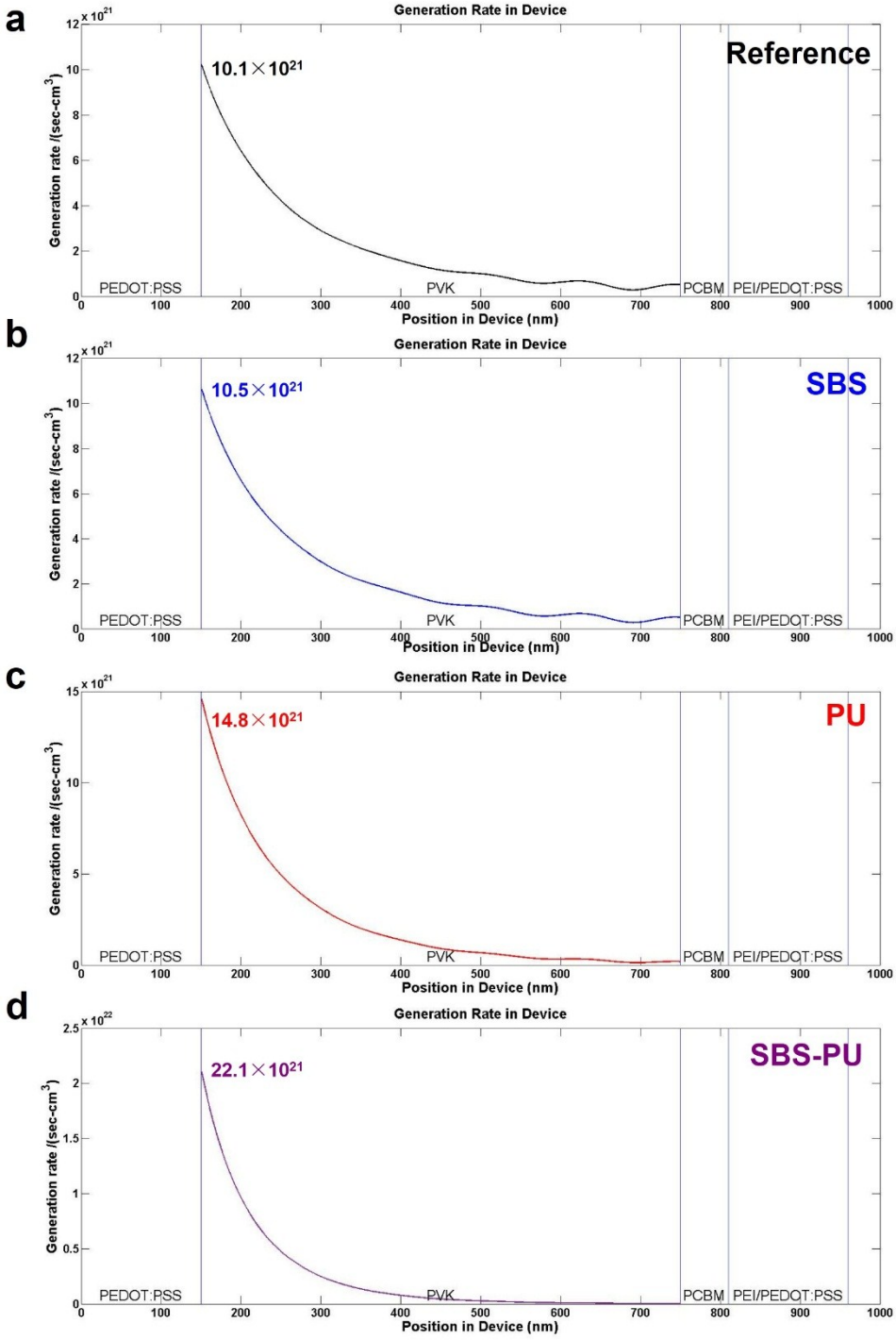

Fig. S9. The simulated carriers' generation rate is based on the optical electric field structure via the transfer matrix method on *Matlab*[3]. The optical refractive index and extinction coefficient of films were analyzed on silicon substrate by an ellipsometer.

It clearly shows that the polymer matrix can improve the carriers' generation rate. The carriers' generation rate of SBS-PU-based devices is nearly twice that of reference devices.

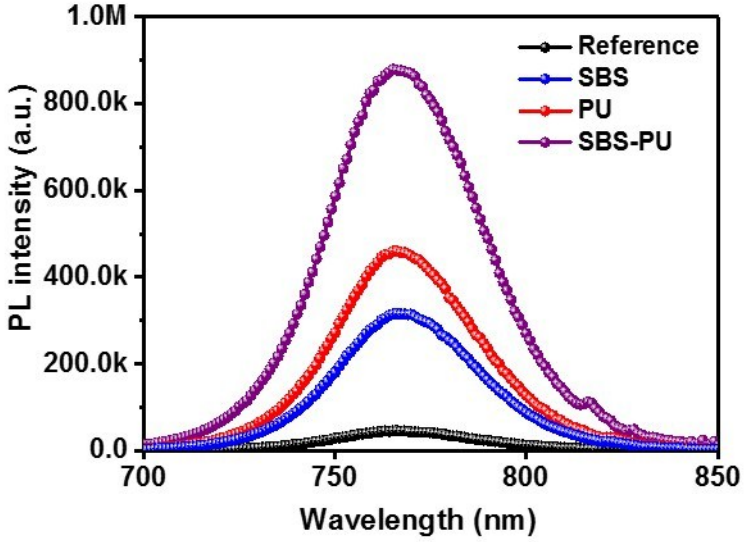

Fig. S10. Photoluminescence of PVK films on PDMS substrate with polymer matrix. A more distinct fluorescence enhancing is observed for SBS-PU-based PVK film.

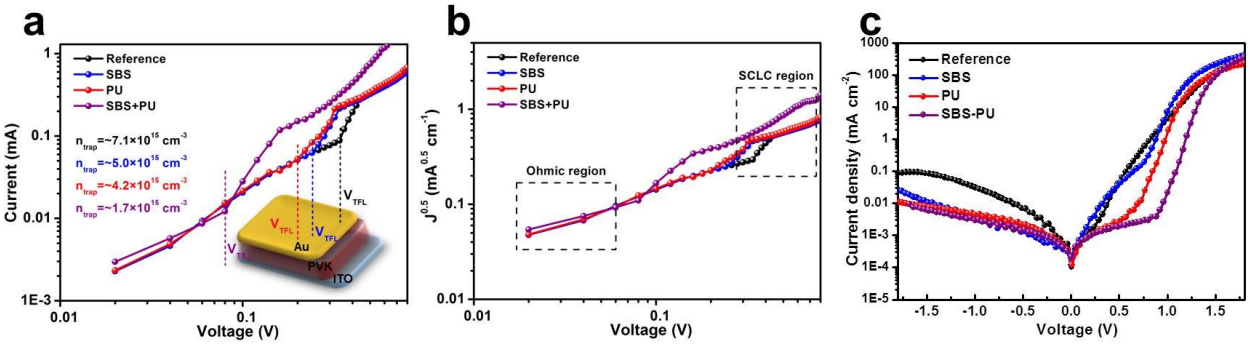

Fig. S11. Current-voltage curves of the PVK films with polymer matrix for space charge limited current (SCLC) analysis[4,5]. The inset depicts the SCLC architecture. (a) The trap density (n_{trap}) of different PVK films. (b) The carrier mobility (μ) of different PVK films. (C) The dark *J*−*V* curves of the device based on different PVK films (the device structure is PDMS/PEDOT:PSS/PVK/PEI/PEDOT:PSS/PDMS).

The trap density (n_{trap}) of PVK films are determined from the SCLC model, using a device of PDMS/PEDOT:PSS/PVK/Au and measuring the current-voltage from 0 V to 1 V. The n_{trap} can be calculated by following equation:

$$n_{trap} = \frac{2V_{tfl}\varepsilon\varepsilon_0}{eL^2}$$

where *e* (1.6×10^{-19}) is the elementary charge, *L* (~600 nm) is the thickness of PVK films, ε is the relative dielectric constant of PVK films (~68, determined by the impedance spectroscopy), ε_0 is the vacuum dielectric constant and V_{tfl} is the trap-filled limited voltage. The V_{tfl} value of reference, SBS, PU and SBS-PU devices is 0.34 V, 0.24 V, 0.20 V and 0.08 V, respectively. So the calculated n_{trap} of reference, SBS, PU and SBS-PU devices is ~7.1×10^{-15} cm^{-3}, ~5.0×10^{-15} cm^{-3}, ~4.2×10^{-15} cm^{-3} and ~1.7×10^{-15} cm^{-3}, respectively.

In addition, the carrier mobility (μ) can be determined according to the Mott−Gurney law:

$$\mu = \frac{8JL^3}{9V^2\varepsilon\varepsilon_0}$$

where *J* is the current density, and the effective area is 1.01 cm^2. The calculated μ of reference, SBS, PU and SBS-PU devices is 2.2×10^{-4} cm^2 V^{-1} S^{-1}, 2.6×10^{-4} cm^2 V^{-1} S^{-1}, 3.0×10^{-4} cm^2 V^{-1} S^{-1} and 1.1×10^{-3} cm^2 V^{-1} S^{-1}, respectively.

To further determine the quality of the PVK films, the dark current−voltage (*J*−*V*)

characteristics for the devices based on different PVK films are presented in Fig. S11c. The much lower dark current density of the devices with SBS-PU matrix means enlarged shunt resistance, restrained leakage current, and higher rectification ratio, which also prove less defects and recombination centers with the biomimetic crystallization[6].

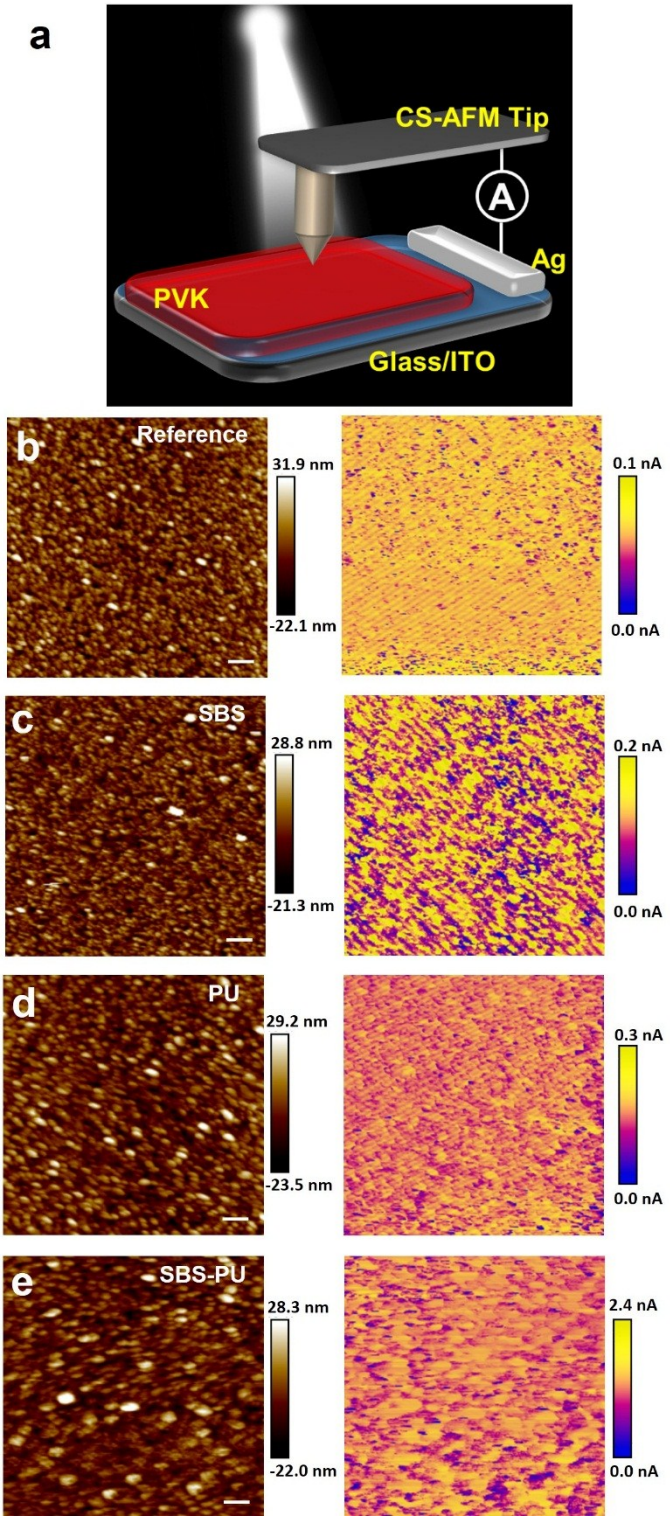

Fig. S12. Current-sensing (CS) AFM measurements. (a) Diagram of testing structure: The PVK sample surface is illuminated while a conductive AFM tip measures the photocurrent with an applied bias of 6 V. (b) Corresponding height AFM images (all scale bar, 1 μm) and c, Current-sensing AFM images of various PVK films on Glass/ITO substrate.

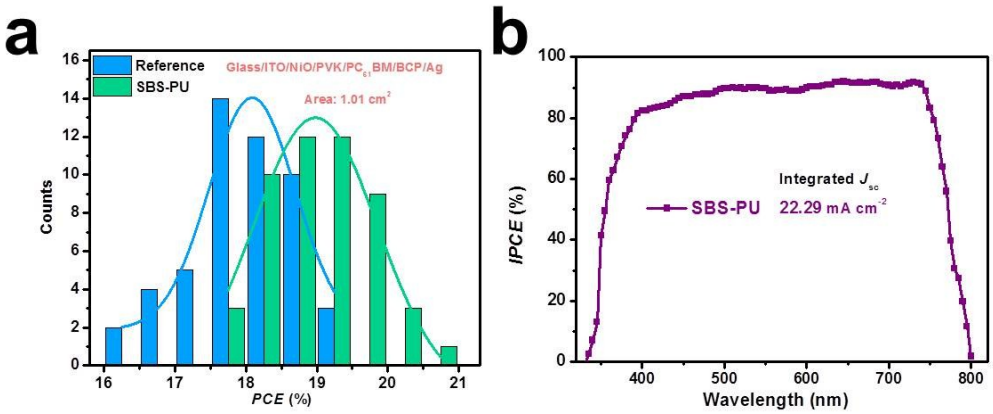

Fig. S13. Universality of the biomimetic crystallization on rigid substrate. (a) Performance distribution of the reference and SBS-PU-based rigid devices for 50 samples in five batches. (b) The corresponding IPCE spectra of the rigid PSCs.

The rigid devices were prepared according to our previous report[1,7]. The structure of devices is Glass/ITO/NiO/PVK/$PC_{61}BM$/BCP/Ag. The NiO_x ink was spin-coated on pre-clean Glass/ITO electrode, then thermal annealing to obtain the HTL. The PVK films were deposited as the same method with the wearable devices. The $PC_{61}BM$ layer was modified by bathocuproine before vacuum evaporating the Ag electrode. The effective area was 1.01 cm^2 defined by the certified mask. The measurement conditions were in agreement with the wearable devices.

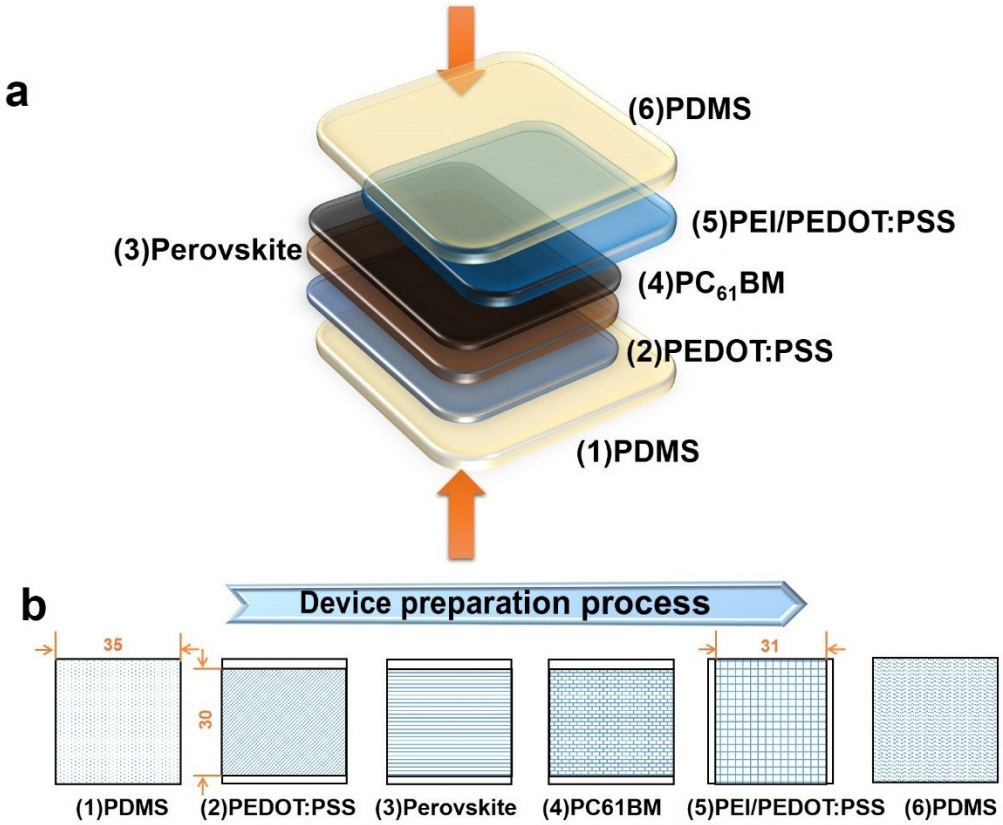

Fig. S14. (a) Configuration of the wearable PSCs and semi-transparent property. (b) Device preparation process of the wearable PSCs from the bottom substrate to top passivation layer, the unit of length is millimeter.

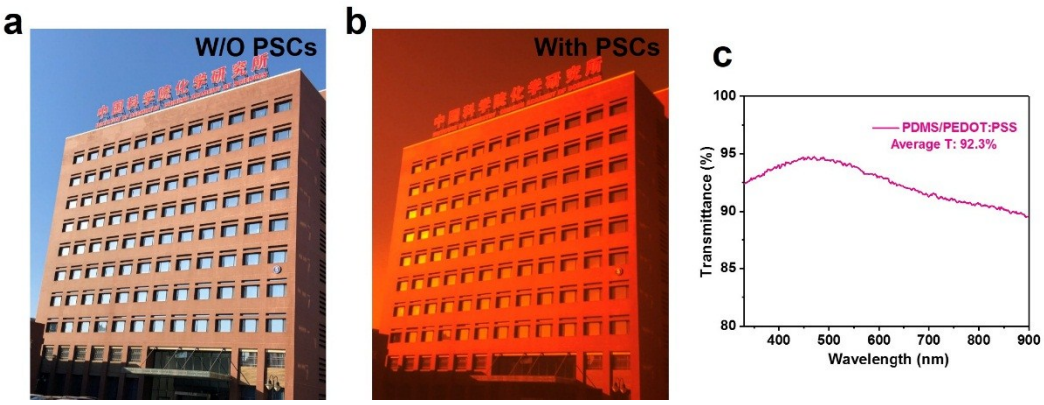

Fig. S15. Photographs are (a) not taken through and (b) taken through the SBS-PU-based PSCs. The PSCs are attached to the camera. The two photographs verify a certain amount of semi-transparency of the wearable PSCs (The photographs are taken by Xiaotian Hu). (c) The transmittance of PDMS/PEDOT:PSS electrode (Average T: 92.3%).

Tab. S1. Averaged photovoltaic parameters of wearable PSCs with different matrix. Data in the parentheses indicate the maximum value. All the average values are calculated by at least fifty samples.

Device	J_{sc} (mA cm^{-2})	V_{oc} (V)	FF	PCE (%)	Integrated J_{sc} (mA cm^{-2})
Reference	13.86 (14.55)	1.01(1.04)	0.57(0.62)	7.98(9.38)	14.51
SBS	15.92(16.45)	1.03(1.05)	0.65(0.70)	10.36(12.09)	16.04
PU	16.32(16.74)	1.03(1.05)	0.68(0.71)	11.66(12.48)	16.43
SBS-PU	18.46(18.70)	1.06(1.07)	0.76(0.78)	15.01(15.61)	18.07

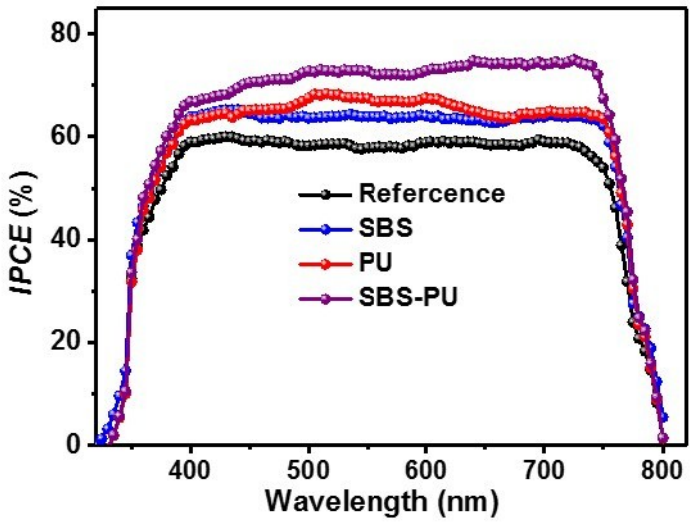

Fig. S16. The corresponding IPCE spectra of the wearable PSCs.

Tab. S2. Photovoltaic parameters of SBS-PU-based devices from ten batches of devices counting 100 cells in total (both the results of the backward and forward directions are included).

Sample No.	J_{sc} (mA cm^{-2})	V_{oc} (V)	FF	PCE (%)	Sample No.	J_{sc} (mA cm^{-2})	V_{oc} (V)	FF	PCE (%)
1	18.50	1.07	0.77	15.24	**51**	18.35	1.07	0.77	15.12
2	18.70	1.06	0.78	15.46	**52**	18.43	1.06	0.77	15.04
3	18.47	1.06	0.77	15.07	**53**	18.70	1.06	0.74	14.67
4	18.57	1.05	0.72	14.04	**54**	18.46	1.07	0.78	15.40
5	18.34	1.05	0.76	14.64	**55**	18.66	1.07	0.78	15.57
6	18.58	1.06	0.78	15.36	**56**	18.70	1.07	0.78	15.61
7	18.51	1.06	0.78	15.30	**57**	18.37	1.05	0.74	14.28
8	18.69	1.06	0.77	15.25	**58**	18.59	1.07	0.77	15.32
9	17.98	1.07	0.78	15.01	**59**	18.58	1.06	0.76	14.97
10	18.70	1.06	0.77	15.26	**60**	18.27	1.07	0.76	14.85
11	18.08	1.07	0.74	14.31	**61**	18.58	1.06	0.76	14.97
12	18.16	1.07	0.77	14.96	**62**	18.64	1.06	0.71	14.03
13	18.67	1.07	0.77	15.38	**63**	18.62	1.07	0.77	15.34
14	18.62	1.07	0.77	15.34	**64**	18.63	1.07	0.78	15.55
15	18.16	1.04	0.77	14.54	**65**	18.16	1.07	0.74	14.38
16	18.56	1.05	0.76	14.81	**66**	18.27	1.07	0.77	15.06
17	18.65	1.07	0.76	15.17	**67**	18.61	1.06	0.78	15.39
18	17.73	1.07	0.78	14.79	**68**	18.70	1.07	0.78	15.61
19	18.59	1.04	0.77	14.89	**69**	18.44	1.06	0.78	15.25
20	18.18	1.07	0.76	14.78	**70**	18.70	1.06	0.76	15.06
21	18.38	1.07	0.72	14.16	**71**	18.66	1.07	0.78	15.57
22	18.55	1.07	0.77	15.28	**72**	18.19	1.05	0.74	14.14
23	17.87	1.06	0.73	13.83	**73**	18.35	1.07	0.78	15.31
24	17.75	1.07	0.75	14.24	**74**	18.63	1.07	0.78	15.55
25	18.61	1.07	0.78	15.53	**75**	18.64	1.06	0.74	14.62
26	18.70	1.07	0.78	15.61	**76**	18.61	1.05	0.75	14.65
27	18.37	1.05	0.73	14.08	**77**	18.59	1.07	0.73	14.52
28	18.47	1.07	0.78	15.41	**78**	18.31	1.07	0.77	15.08
29	18.19	1.07	0.78	15.18	**79**	18.66	1.07	0.75	14.97
30	18.21	1.06	0.75	14.48	**80**	18.26	1.06	0.73	14.13
31	18.59	1.07	0.73	14.52	**81**	18.36	1.07	0.78	15.33
32	18.52	1.07	0.78	15.46	**82**	18.59	1.07	0.75	14.92
33	18.62	1.06	0.73	14.41	**83**	18.63	1.07	0.77	15.35
34	18.31	1.07	0.75	14.70	**84**	18.66	1.07	0.75	14.97
35	18.50	1.07	0.76	15.04	**85**	18.61	1.07	0.77	15.33
36	18.63	1.07	0.76	15.15	**86**	18.05	1.07	0.72	13.91
37	18.66	1.06	0.77	15.23	**87**	18.70	1.07	0.77	15.41
38	18.64	1.06	0.76	15.02	**88**	18.61	1.06	0.77	15.19

39	18.62	1.07	0.78	15.54	**89**	18.69	1.07	0.74	14.80
40	18.49	1.07	0.78	15.43	**90**	18.59	1.06	0.77	15.17
41	18.68	1.07	0.78	15.59	**91**	18.03	1.07	0.77	14.85
42	18.09	1.07	0.76	14.71	**92**	18.61	1.07	0.73	14.54
43	18.70	1.06	0.76	15.06	**93**	18.43	1.06	0.78	15.24
44	18.04	1.07	0.77	14.86	**94**	18.66	1.06	0.77	15.23
45	18.33	1.07	0.77	15.10	**95**	18.62	1.07	0.75	14.94
46	18.68	1.07	0.77	15.39	**96**	18.62	1.06	0.77	15.20
47	17.92	1.05	0.72	13.55	**97**	18.64	1.07	0.77	15.36
48	18.43	1.07	0.77	15.19	**98**	18.62	1.07	0.78	15.54
49	18.57	1.06	0.76	14.96	**99**	18.68	1.07	0.78	15.59
50	18.20	1.06	0.72	13.89	**100**	18.35	1.07	0.76	14.92

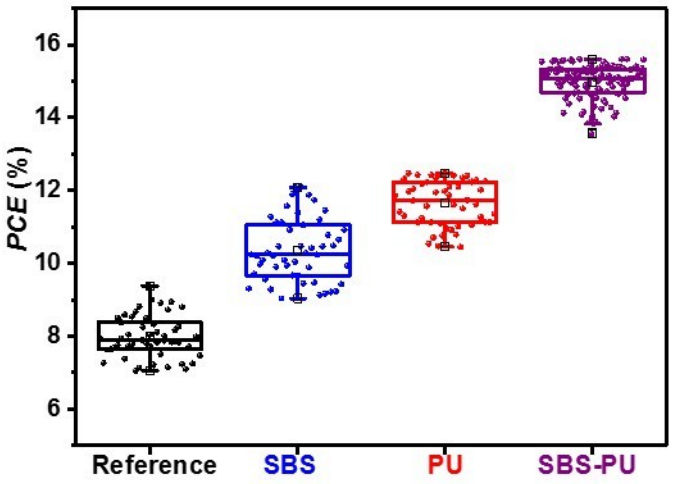

Fig. S17. Statistics of the device performance. In the boxplots, the open square represents the maximum, minimum and mean values.

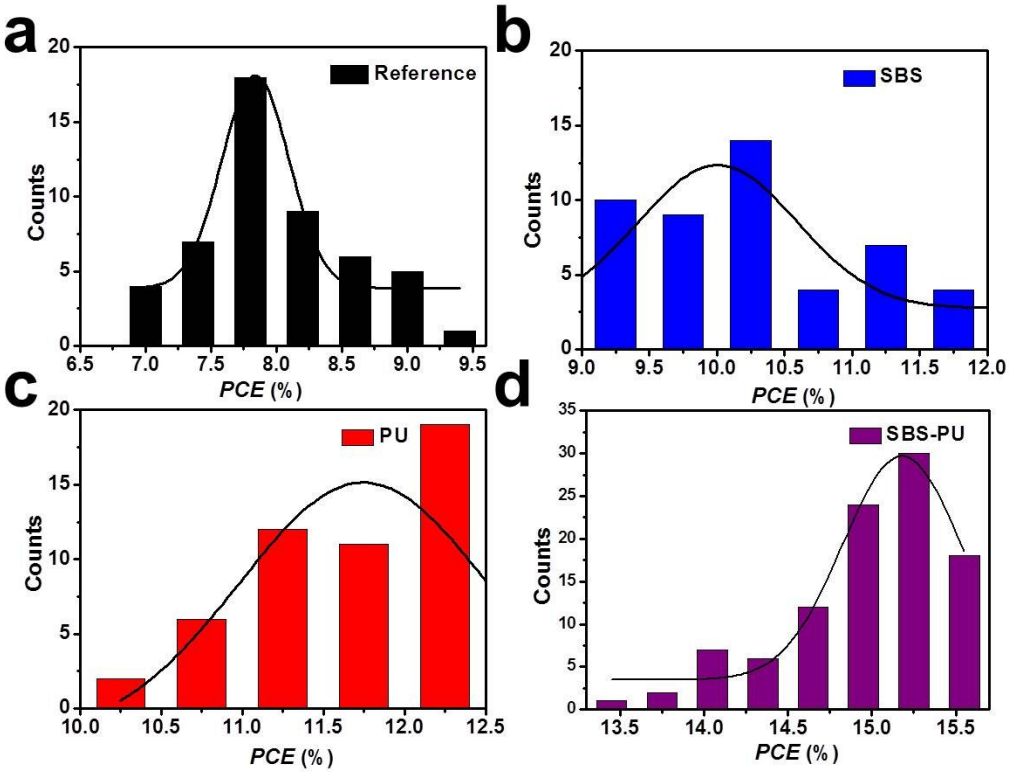

Fig. S18. Performance distribution of wearable devices with (a) Reference, (b) SBS, (c) PU and (d) SBS-PU.

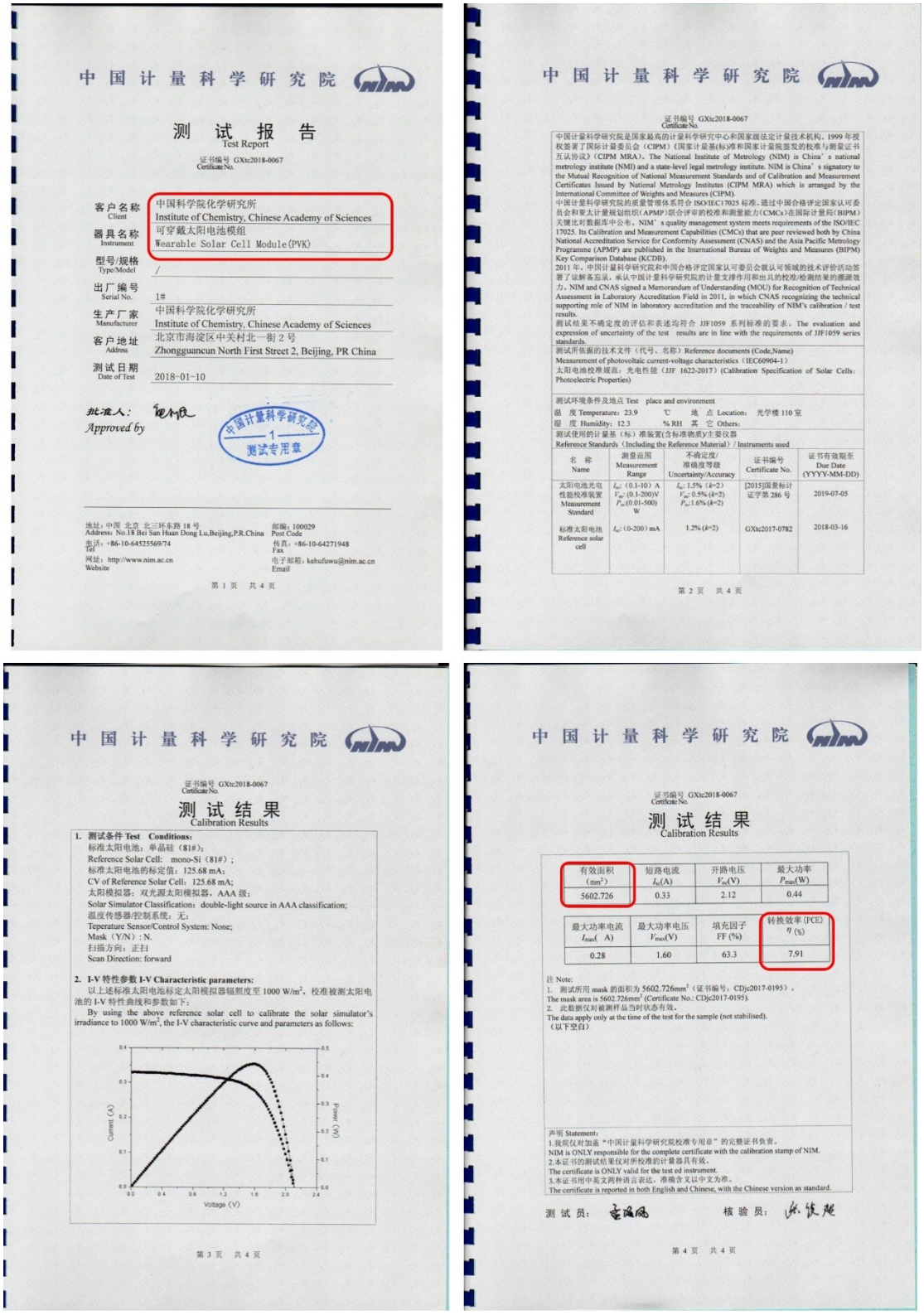

中国计量科学研究院

测 试 报 告
Test Report

证书编号 GXtc2018-0067
Certificate No.

客户名称 Client	中国科学院化学研究所 Institute of Chemistry, Chinese Academy of Sciences
器具名称 Instrument	可穿戴太阳电池模组 Wearable Solar Cell Module(PVK)
型号/规格 Type/Model	/
出厂编号 Serial No.	1#
生产厂家 Manufacturer	中国科学院化学研究所 Institute of Chemistry, Chinese Academy of Sciences
客户地址 Address	北京市海淀区中关村北一街2号 Zhongguancun North First Street 2, Beijing, PR China
测试日期 Date of Test	2018-01-10

批准人：
Approved by

中国计量科学研究院 1 测试专用章

地址：中国 北京 北三环东路18号 Address: No.18 Bei San Huan Dong Lu,Beijing,P.R.China
邮编：100029 Post Code
电话：+86-10-64525569/74 Tel
传真：+86-10-64271948 Fax
网址：http://www.nim.ac.cn Website
电子邮箱：kehufuwu@nim.ac.cn Email

第 1 页 共 4 页

中国计量科学研究院

证书编号 GXtc2018-0067
Certificate No.

中国计量科学研究院是国家最高的计量科学研究中心和国家级法定计量技术机构，1999年授权签署了国际计量委员会（CIPM）《国家计量基(标)准和国家计量院签发的校准与测量证书互认协议》(CIPM MRA)。The National Institute of Metrology (NIM) is China's national metrology institute (NMI) and a state-level legal metrology institute. NIM is China's signatory to the Mutual Recognition of National Measurement Standards and of Calibration and Measurement Certificates Issued by National Metrology Institutes (CIPM MRA) which is arranged by the International Committee of Weights and Measures (CIPM).
中国计量科学研究院的质量管理体系符合 ISO/IEC17025 标准，通过中国合格评定国家认可委员会和亚太计量规划组织(APMP)联合评审的校准和测量能力(CMCs)在国际计量局(BIPM)关键比对数据库中公布。NIM's quality management system meets requirements of the ISO/IEC 17025. Its Calibration and Measurement Capabilities (CMCs) that are peer reviewed both by China National Accreditation Service for Conformity Assessment (CNAS) and the Asia Pacific Metrology Programme (APMP) are published in the International Bureau of Weights and Measures (BIPM) Key Comparison Database (KCDB).
2011年，中国计量科学研究院和中国合格评定国家认可委员会就认可领域的技术评价活动签署了谅解备忘录，承认中国计量科学研究院的计量支撑作用和出具的校准/检测结果的溯源效力。NIM and CNAS signed a Memorandum of Understanding (MOU) for Recognition of Technical Assessment in Laboratory Accreditation Field in 2011, in which CNAS recognizing the technical supporting role of NIM in laboratory accreditation and the traceability of NIM's calibration / test results.
测试结果不确定度的评估和表述均符合 JJF1059 系列标准的要求。The evaluation and expression of uncertainty of the test results are in line with the requirements of JJF1059 series standards.

测试所依据的技术文件（代号、名称）Reference documents (Code,Name)
Measurement of photovoltaic current-voltage characteristics（IEC60904-1）
太阳电池校准规范：光电性能（JJF 1622-2017）(Calibration Specification of Solar Cells: Photoelectric Properties)

测试环境条件及地点 Test place and environment
温 度 Temperature：23.9 ℃ 地 点 Location：光学楼 110 室
湿 度 Humidity：12.3 % RH 其 它 Others：

测试使用的计量基（标）准装置(含标准物质)/主要仪器
Reference Standards（Including the Reference Material）/ Instruments used

名 称 Name	测量范围 Measurement Range	不确定度/准确度等级 Uncertainty/Accuracy	证书编号 Certificate No.	证书有效期至 Due Date (YYYY-MM-DD)
太阳电池光电性能校准装置 Measurement Standard	I_{sc}: (0.1-10) A V_{oc}: (0.1-200)V P_{m}:(0.01-500) W	I_{sc}: 1.5%（k=2） V_{oc}: 0.5% (k=2) P_{m}:1.6% (k=2)	[2015]国量标计证字第 286 号	2019-07-05
标准太阳电池 Reference solar cell	I_{sc}: (0-200) mA	1.2% (k=2)	GXtc2017-0782	2018-03-16

第 2 页 共 4 页

中国计量科学研究院

证书编号 GXtc2018-0067
Certificate No.

测 试 结 果
Calibration Results

1. 测试条件 Test Conditions:
标准太阳电池：单晶硅（81#）;
Reference Solar Cell: mono-Si（81#）;
标准太阳电池的标定值：125.68 mA;
CV of Reference Solar Cell: 125.68 mA;
太阳模拟器：双光源太阳模拟器，AAA 级;
Solar Simulator Classification: double-light source in AAA classification;
温度传感器/控制系统：无;
Teperature Sensor/Control System: None;
Mask（Y/N）: N.
扫描方向：正扫
Scan Direction: forward

2. I-V 特性参数 I-V Characteristic parameters:
以上述标准太阳电池标定太阳模拟器辐照度至 1000 W/m^2，校准被测太阳电池的 I-V 特性曲线和参数如下：
By using the above reference solar cell to calibrate the solar simulator's irradiance to 1000 W/m^2, the I-V characteristic curve and parameters as follows:

第 3 页 共 4 页

中国计量科学研究院

证书编号 GXtc2018-0067
Certificate No.

测 试 结 果
Calibration Results

有效面积 (mm^2)	短路电流 I_{sc}(A)	开路电压 V_{oc}(V)	最大功率 P_{max}(W)
5602.726	0.33	2.12	0.44

最大功率电流 I_{max}(A)	最大功率电压 V_{max}(V)	填充因子 FF (%)	转换效率(PCE) η (%)
0.28	1.60	63.3	7.91

注 Note:
1. 测试所用 mask 的面积为 5602.726mm^2（证书编号：CDjc2017-0195）。
The mask area is 5602.726mm^2 (Certificate No.: CDjc2017-0195).
2. 此数据仅对被测样品当时状态有效。
The data apply only at the time of the test for the sample (not stabilised).
（以下空白）

声明 Statement:
1.我院仅对加盖"中国计量科学研究院校准专用章"的完整证书负责。
NIM is ONLY responsible for the complete certificate with the calibration stamp of NIM.
2.本证书的测试结果仅对所校准的计量器具有效。
The certificate is ONLY valid for the test ed instrument.
3.本证书用中英文两种语言表达，准确含义以中文为准。
The certificate is reported in both English and Chinese, with the Chinese version as standard.

测 试 员： 核 验 员：

第 4 页 共 4 页

Fig. S19. Original reports of the wearable PVK module certificate results by the National Institute of Metrology (NIM) of China. The module area is measured at 56.02 cm^2 with a PCE of 7.91%.

Tab. S3. Several representative performances of flexible PSCs for comparison to this work.

Configuration	Notes	Device chip (PCE %; area cm^2)		Module (PCE %; area cm^2)		Ref.
PET/ITO/PTAA	Composition-Tailored PVK	14.0-16.0 (18.1 best)	0.1	-	-	Adv. Mater., 2017, 29, 1605900
PET/ITO/ETL/…	$Pb(SCN)_2$ additive	17.96 (best)	0.08	-	-	Nano Energy, 2017, 35, 223–232.
PEN/ITO/SnO_2/…	SnO_2 QD	16.97 (best)	0.09	-	-	Adv. Mater., DOI: 10.1002/adma.201706023
PET/ITO/ETL	ionic liquid ETL	16.0	0.08	-	-	Adv. Mater., 2016, 28, 5206-5213.
PEN/ITO/PTAA/…	ZnO ETL	15.6	0.16	-	-	J. Mater. Chem. A, 2016, 4, 1572-1578.
PEN/ITO/Zn_2SnO_4/…	Zn_2SnO_4 ETL	15.3	0.10	-	-	Nat. Commun., 2015, 6, 7410.
PEN/Graphene-MoO_3/…	Graphene electrode	15.0	0.09	-	-	Energy Environ. Sci., 2017, 10, 337
PET/Ag mesh /PEDOT:PSS/…	Ultralight device	14.0	0.1	-	-	Nat. Commun., 2016, 7, 10214.
PEN/ITO/Zn_2SnO_4	Low temperature process	13.7	0.10	-	-	Nat. Commun., 2015, 6, 7410.
PET/ITO/NiO_x/…	NiO_x nanoparticles ink	13.4	0.07	-	-	ACS Nano, 2016, 10, 3630−3636.
PET/ITO/NiO_x/…	nanostructured HTL	13.3	0.06	-	-	ACS Nano, 2016, 10, 1503−1511.
PET/ITO /PEDOT:PSS/…	layer by layer perovskite	12.3	0.12	-	-	Adv. Mater., 2015, 27, 1053-1059.
PEN/ITO/TiO_x	ALD TiO_x	12.2	-	-	-	Energy Environ. Sci., 2015, 8, 916
PI/ In_2O_3:H/ PTAA/PVK/…	semi-transparent	9%	0.29	-	-	Nat. Energy, 2017, 2, 16190.
PET/hc-PEDOT:PSS/…	ultrathin substrate	12.5	0.15	~8.4	8.64	Nat. Mater., 2015, 14, 1032-1039.
PEN/ITO/C_{60}/...	PbI_2 vacuum deposition	11.6	1.20	7.8	16.00	Sci. Rep. 2018, 8, 442.
PDMS/PEDOT:PSS/ PVK/PEI/ PEDOT:PSS/PDMS	**Wearable; Stretchable**	**15.0**	**1.01**	**7.9 (certified)**	**56.02**	**This work**

*The values of PCE are usually referred to the average PCE. "-"means not mentioned. HTL and ETL are hole transport layer and electron transport layer, respectively.

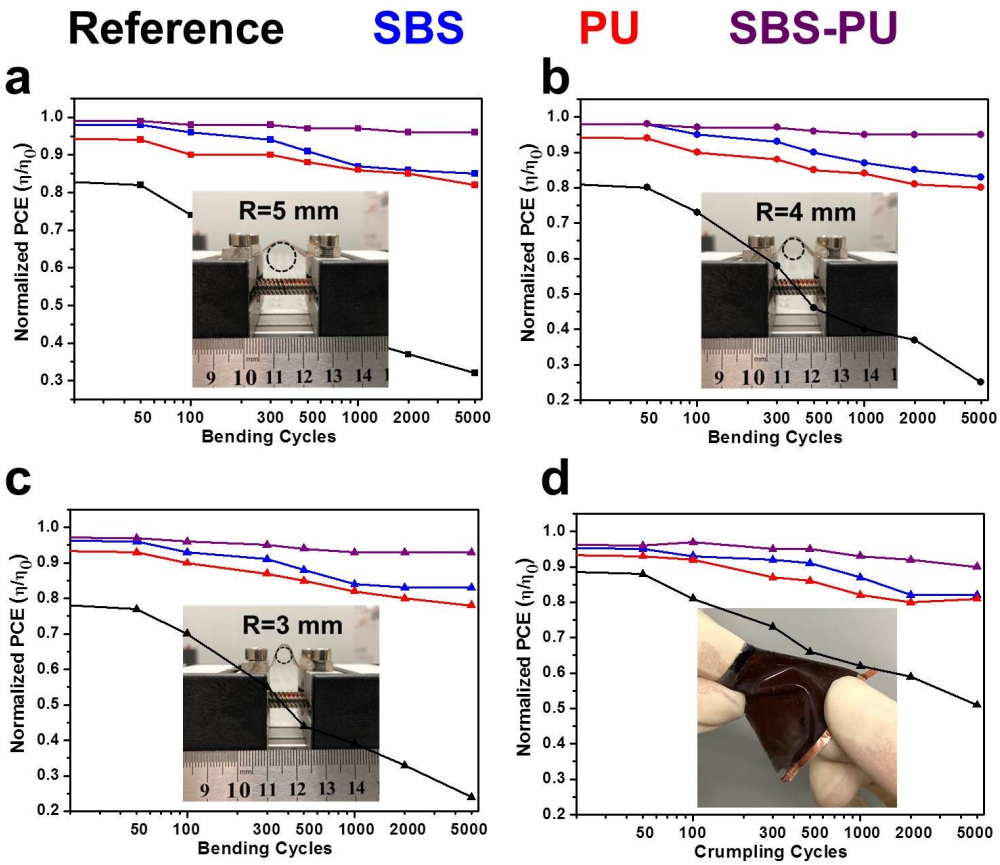

Fig. S20. Normalized average PCE of PSCs as a function of bending cycles with radius of (a) 5 mm, (b) 4 mm and (c) 3 mm, respectively. (d) Normalized average PCE of PSCs under crumpling test for 5000 cycles.

Dynamical mechanics simulation

To investigate the mechanical stability of different perovskite films, we used the finite-element method to simulate the deformation of perovskite films under bending and stretching. Due to the thickness of functional layers is much thinner than that of PDMS. The PDMS layers are omitted under vertical bending and the stretching model is defined as an elastomer under horizontal stretching.

Firstly, the basic theories for finite-element simulation were discussed.

The bending test: For the multilayer films, the relationship between film stress and curvature radius is shown in: equation (**1**)

$$\sigma_f = \frac{E_f h_f^2}{6(1 - v_s)R} \qquad (\mathbf{1})$$

σ_f is the value of stress, E_f is the Young's modulus of film, h_f is the thickness of film, v_s is the poisson's ratio of film and R is curvature radius.

The relationship of film stress and displacement: equation (**2**)

$$D_{ij} = \sum_{k=1}^{n} \int_{z_k}^{z_k + h_k} Q_{ij}^{(k)} z^2 dz \qquad (\mathbf{2})$$

Where D_{ij} is bending rigidity of system, k is the number of films and Q_{ij} is strain under stress of *k* film. We can write the general control equation of film stress and deformational displacement: as equation (**3**)

$$D_{11}\frac{\partial^4 w}{\partial x^4} + 2(D_{12} + 2D_{23})\frac{\partial^4 w}{\partial x^2 \partial y^2} + D_{22}\frac{\partial^4 w}{\partial y^4} - N_x\frac{\partial^2 w}{\partial x^2} - N_y\frac{\partial^2 w}{\partial y^2} - 2N_{xy}\frac{\partial^2 w}{\partial x \partial y} = \frac{\partial^2}{\partial x^2}(N_x)\frac{h}{2} + 2\frac{\partial^2}{\partial x \partial y}(N_{xy})\frac{h}{2} + \frac{\partial^2}{\partial y^2}(N_y)\frac{h}{2}$$

(**3**)

The stretching test: The tension of each layer and displacement: as equation (**4**)

$$\frac{F}{S} = E_f \frac{\Delta l}{l_0} \qquad (\mathbf{4})$$

Where F is tension, S is cross-sectional area of film, E_f is the Young's modulus of film, Δl is displacement and l_0 is length of film.

The corresponding mechanical finite-element simulations: The Young's modulus of different perovskite and PEDOT:PSS films is obtained from force-separation curves

by AFM, as shown in Fig. S21. The other mechanical properties were obtained from the Poisson's ratio tester (DP-4/2) or references[8-10]. All the mechanical properties of films are summarized in Tab. S4.

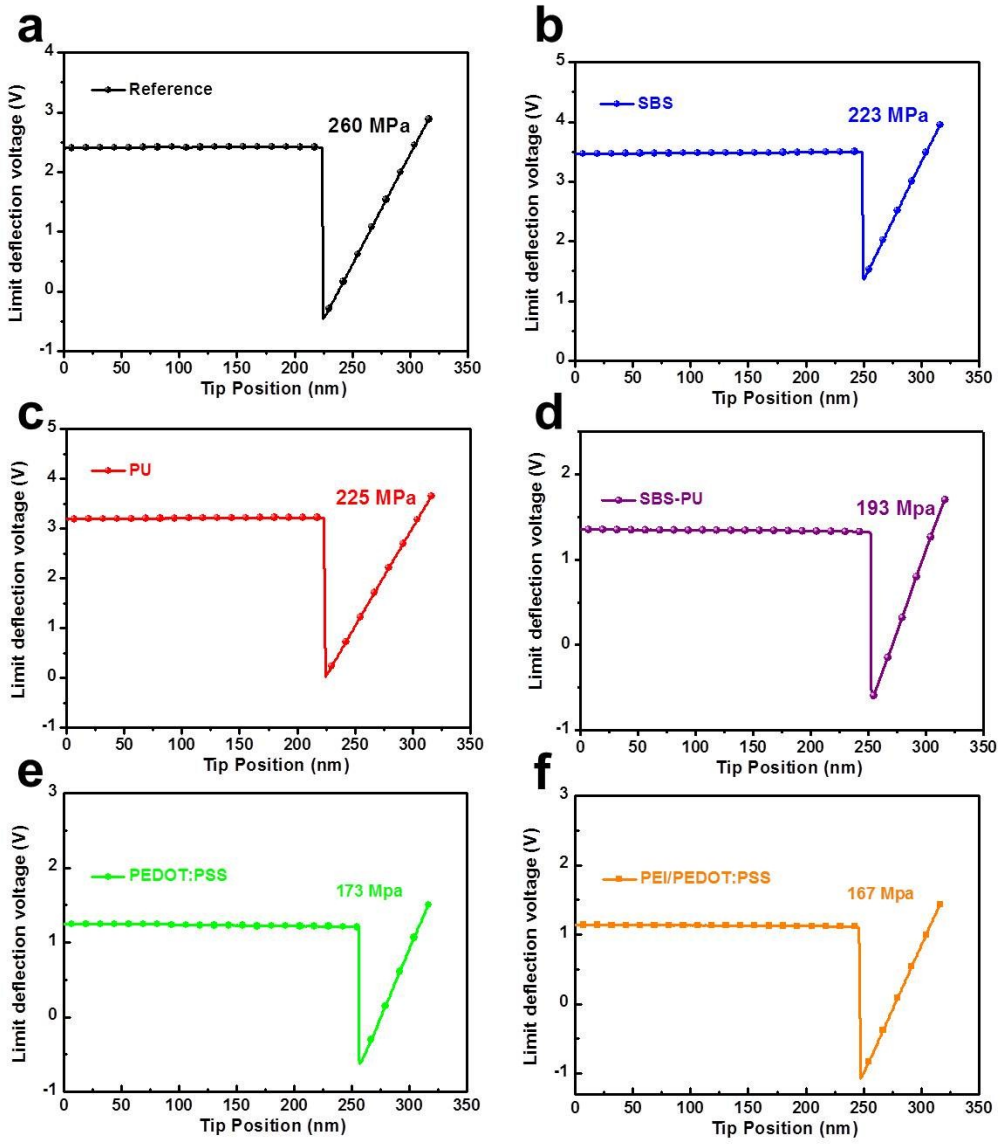

Fig. S21. Limit deflection curves of (a-d) different PVK films and (e,f) PEDOT:PSS films.

Tab. S4. Mechanical properties of each functional film for finite-element simulation.

Materials	Thickness (μm)	Young's modulus (Mpa)	Density (ρ, g cm^{-3})	Poisson's ratio
PEDOT:PSS	0.15	173	1.39	0.32
PVK	0.60	260;223; 225;193	4.1	0.31
$PC_{61}BM$	0.06	385	1.6	0.36
PEI/ PEDOT:PSS	0.13	167	1.37	0.32

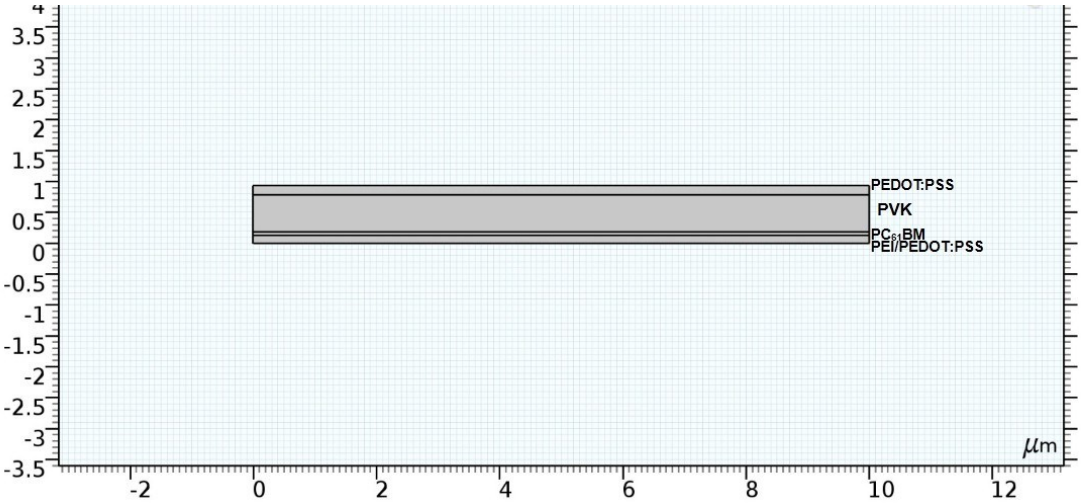

Fig. S22. The geometric model of PSCs for bending and stretching simulation. The design of this two dimensional model is proportional, and the size of geometric unit is 0.5 μm which can match with the grain size of PVK films.

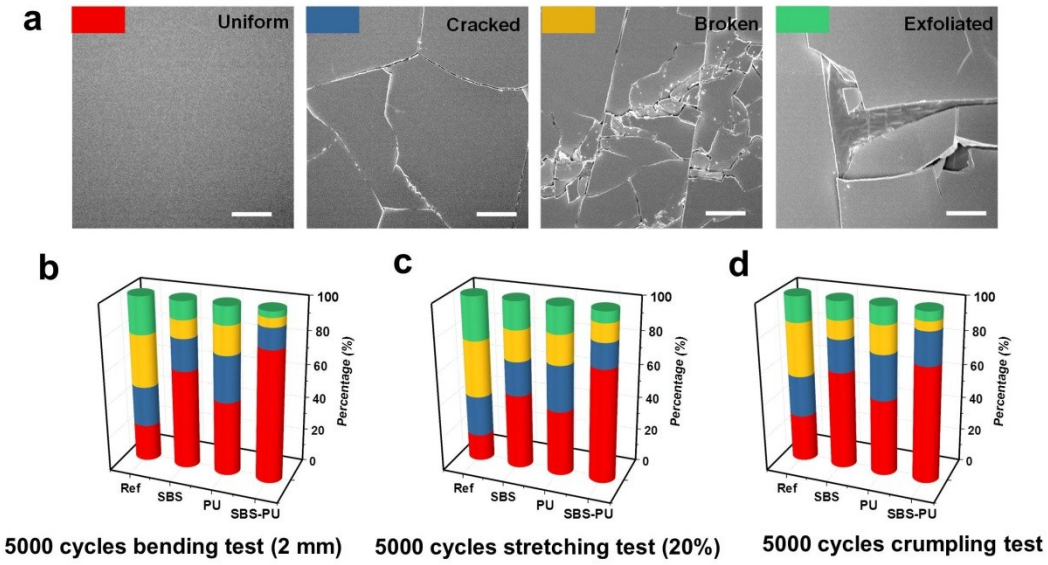

Fig. S23. Statistics of the mechanical stability. (a) Four distinct mechanical morphology of SEM results by bending or stretching test on wearable PSCs. Red is uniform, blue is cracked, yellow is broken and green is exfoliated ones. (b) Stacked column of the corresponding frequency of the PSCs after 5000 cycles bending test. (c) Stacked column of the corresponding frequency of the PSCs after 5000 cycles stretching test. (d) Stacked column of the corresponding frequency of the PSCs after 5000 cycles crumpling test. Both of the statistics are over 100 views.

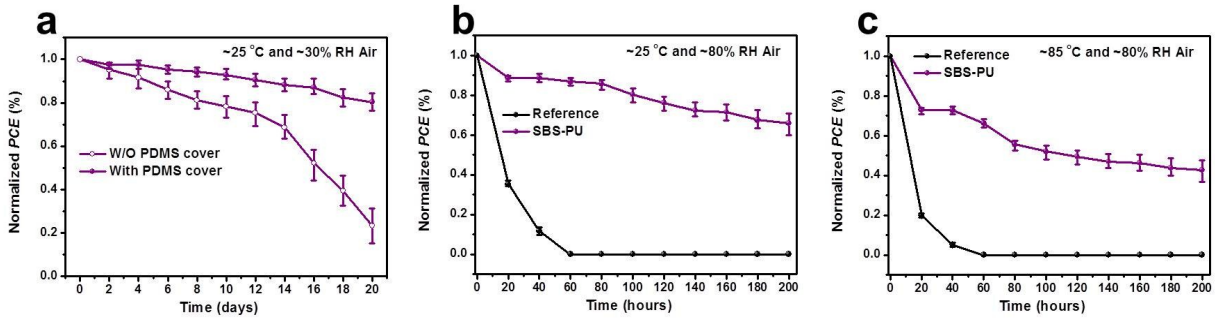

Fig. S24. Long-term stability. (a) The PSCs W/O or with PDMS cover under ~25 °C and ~30% relative humidity (RH) conditions in the air. The device W/O PDMS cover is peeling off the PDMS after film-transfer lamination. (b) The PSCs with PDMS cover under the humid long-term stability test (~25 °C and ~80% RH). (c) The PSCs with PDMS cover under the thermal long-term stability test (~85 °C and ~80% RH). All the PSCs are stored in dark condition.

The top PDMS serves as a passivation for the device encapsulation, leading to an enhanced long-term stability as shown in Fig. S24a. Moreover, the PSCs with SBS-PU matrix can improve the humid and thermal long-term stability, which could be attributed to the surface SBS layer on the PVK film and high quality of PVK film with this biomimetic crystallization. The results show evident improvement of long-term stability with different humid and thermal conditions.

Movie S1. The video shows the wearable PSCs power source can charge a smartwatch in a variety of body movements (~20 klx solar irradiance).

Movie S2. The video shows different PVK films on Glass/PDMS/PEDOT:PSS substrate during initial crystallization at 100 ^{o}C via the high-speed camera.

References

1. Z. Huang, X. Hu, C. Liu, L. Tan and Y. Chen, *Adv. Funct. Mater.*, 2017, **27**, 1703061.
2. D. Bi, C. Yi, J. Luo, J. D. Décoppet, F. Zhang, S. M. Zakeeruddin, X. Li, A. Hagfeldt and M. Grätzel, *Nat. Energy*, 2016, **1**, 16142.
3. G. F. Burkhard, E. T. Hoke and M. D. McGehee, *Adv. Mater.*, 2010, **22**, 3293–3297.
4. Q. Han, S.-H. Bae, P. Sun, Y.-T. Hsieh, Y. M. Yang, Y. S. Rim, H. Zhao, Q. Chen, W. Shi, G. Li and Y. Yang, *Adv. Mater.*, 2016, **28**, 2253–2258.
5. M. He, B. Li, X. Cui, B. Jiang, Y. He, Y. Chen, D. O'Neil, P. Szymanski, M. A. Ei-Sayed, J. Huang and Z. Lin, *Nat. Commun.*, 2017, **8**, 16045.
6. H. Zhang, H. Wang, W. Chen and A. K. Y. Jen, *Adv. Mater.*, 2017, **29**, 201604984.
7. X. Hu, Z. Huang, X. Zhou, P. Li, Y. Wang, Z. Huang, M. Su, W. Ren, F. Li, M. Li, Y. Chen and Y. Song, *Adv. Mater.*, 2017, **29**, 1703236
8. Y. Rakita, S. R. Cohen, N. K. Kedem, G. Hodes and D. Cahen, *MRS Commun.*, 2015, **5**, 623–629.
9. M. Spina, A. Karimi, W. Andreoni, C. A. Pignedoli, B. Náfrádi, L. Forró and E. Horváth, *Appl. Phys. Lett.*, 2017, **12**, 121903.
10. D. Tank, H. H. Lee and D. Y. Khang, *Macromolecules*, 2009, **42**, 7079–7083.